Tuning of collagen scaffold properties modulates embedded endothelial cell regulatory phenotype in repair of vascular injuries *in vivo*

Dr. Shimon Unterman,
Institute for Medical Engineering and Science, Massachusetts Institute of Technology, Cambridge, MA 02139, USA

Alina Freiman,
Institute for Medical Engineering and Science, Massachusetts Institute of Technology, Cambridge, MA 02139, USA. Ort Braude College, Karmiel, Israel

Margarita Beckerman,
Institute for Medical Engineering and Science, Massachusetts Institute of Technology, Cambridge, MA 02139, USA. Ort Braude College, Karmiel, Israel

Dr. Eytan Abraham,
Institute for Medical Engineering and Science, Massachusetts Institute of Technology, Cambridge, MA 02139, USA. Cardiovascular Division, Department of Medicine, Brigham and Women's Hospital, Harvard Medical School, Boston, MA 02115, USA

Dr. James R.L. Stanley,
CBSET, Inc., Concord Biomedical Sciences and Emerging Technologies, Lexington, MA 02421, USA

Ela Levy,
Institute for Medical Engineering and Science, Massachusetts Institute of Technology, Cambridge, MA 02139, USA. Ort Braude College, Karmiel, Israel

Prof. Natalie Artzi, and
Institute for Medical Engineering and Science, Massachusetts Institute of Technology, Cambridge, MA 02139, USA. Department of Anesthesiology, Brigham and Women's Hospital, Harvard Medical School, Boston, MA 02115, USA

Prof. Elazer Edelman
Institute for Medical Engineering and Science, Massachusetts Institute of Technology, Cambridge, MA 02139, USA. Cardiovascular Division, Department of Medicine, Brigham and Women's Hospital, Harvard Medical School, Boston, MA 02115, USA

Shimon Unterman: unterman@mit.edu; Natalie Artzi: nartzi@mit.edu

Correspondence to: Shimon Unterman, `unterman@mit.edu`; Natalie Artzi, `nartzi@mit.edu`.

NA and EE contributed equally to this work.

Supporting Information
Supporting Information is available from the Wiley Online Library.

Abstract

Perivascularly implantated matrix embedded endothelial cells (MEECs) are potent regulators of inflammation and intimal hyperplasia following vascular injuries. ECs in porous collagen scaffolds adopt a reparative phenotype with significant therapeutic potential. Although the biological effects of MEECs are increasingly understood, less work has studied the tuning of scaffold properties to control cell-substrate interactions and subsequent biological outcomes. We hypothesized that modulating scaffold degradation would change EC phenotype. Scaffolds with differential degradation rates were prepared by crosslinking and pre-degradation. Vascular injury increased degradation and the presence of MEECs retarded injury-mediated degradation. MEECs responded to differential scaffold properties with altered cell viability *in vivo*, suppression of smooth muscle cell (SMC) proliferation *in vitro*, and changes in IL-6 and MMP-9 expression. When implanted perivascularly to a murine carotid wire injury model, tuned scaffolds changed MEEC effects on vascular repair and inflammation. Live animal imaging allowed for real-time tracking of cell viability, inflammation, and scaffold degradation *in vivo*, affording an unprecedented understanding of interactions between cells, substrate, and tissue. MEEC-treated injuries exhibited improved endothelialization and reduced SMC hyperplasia over 14 days. These data demonstrate the potent role material design plays in tuning MEEC efficacy *in vivo*, with implications for the design of clinical therapies.

Keywords

1. Introduction

Cellular therapeutics have been increasingly proposed to treat vascular injuries and sustain the impact of vascular interventions[1]. Endothelial cells (ECs) are regulators of every aspect of vascular biology and when embedded in a matrix can be maintained in a stable regulatory phenotype that has profound effects on vascular repair[2, 3]. Injection of cells without the supporting matrix elicits a significant immune reaction, which is obviated by embedding them in a scaffold. Matrix embedded ECs mimic the secretome of healthy, confluent endothelium in contrast to the secretome of sub-confluent ECs, which can promote disease processes[4]. This regulatory and reparative phenotype is modulated by culture on 3D as opposed to 2D scaffolds[5]. As the endothelial cell secretion profile is modulated by many parameters, embedding endothelial cells within 3D porous polymeric scaffolds stabilizes endothelial cells phenotype by controlling cell-substratum interactions. These matrix embedded endothelial cells (MEECs) have potent effects on regulating the response to vascular injury. Scaffold architecture, cytoskeletal rearrangement and mechanical properties control cell signaling and production of inflammation-modulating cytokines released by these endothelial cells[5, 6, 7]. The unique cascade of events during vascular repair – including inflammation, cellular infiltration, thrombosis, and smooth muscle cell proliferation – precludes a 'one size fits all' approach to material design, and requires that cell-biomaterial therapeutics be tested in a clinically relevant context[3, 8]. Degradable materials offer the opportunity for a greater level of control over cell-material interactions

and insight into dynamic environments. As materials degrade, their physicochemical properties evolve, changing embedded cell behavior and the surrounding tissue state. This can be exploited to control the evolving tissue state and enhance the therapeutic effects of material-cell interactions. Tuning the scaffold degradation rate is often tied to changes in other physicochemical properties of materials including elastic modulus, surface chemistry and ligand density, and porosity. Evaluating how this complex milieu changes in tandem with cell functionality can provide crucial insights into the tripartite relationship between cells, substrate, and the tissue microenvironment

In this study, we modified compressed collagen matrices to exhibit a range of material degradation kinetics, from 'fast-degrading' scaffolds that degrade completely in two weeks to moderate or highly crosslinked 'slow-degrading' scaffolds that only lose ~50% of mass over the same period *in vivo*. We then used these differentially degrading scaffolds to explore embedded cell behavior *in vitro* and *in vivo*. Using *in vivo* imaging technologies, we performed real-time, noninvasive tracking of material degradation, cell viability, and local inflammation [9], and used these data to understand the relationships between material fate, cell viability and healing capacity. We found that degradation rate of scaffolds *in vitro* and *in vivo* was dependent on disease state and cellularity. Vascular injury increased degradation and the presence of cells retarded injury-mediated degradation and further stabilized matrices, possibly due to changes in local inflammation-driven proteolysis. ECs in degradation-tuned scaffolds were able to differentially inhibit SMC proliferation and had altered IL-6 and MMP-9 expression, though most of their biosecretory profiles were unchanged. Finally, we demonstrated treatment with MEECs improved endothelialization and reduced SMC hyperplasia and inflammation in a mouse carotid wire injury model. Conclusions drawn from this study will improve our understanding of the role cell-substrate interactions play in endothelial cell biology. More broadly, they should inform the design of biomaterial carriers for cell therapies.

2. Results

2.1. Control of compressed collagen scaffold degradation in vitro and in vivo is dependent on disease state and ECs

We created a family of materials with a range of degradation kinetics and properties by variably crosslinking or pre-degrading compressed collagen scaffolds. Scaffold degradation varied when immersed without cells in growth media for 10 days (to mimic the *in vitro* cell seeding period prior to *in vivo* implantation), followed by 5 days in collagenase-containing media (to mimic exposure to endogenous proteases following *in vivo* implantation) (Figure 1A). Slow, standard and fast degrading matrices lost 10, 30 and 40%, respectively, of their mass over 10 days. While collagenase had no impact on the slow degrading materials, degradation of standard matrices increased substantially and fast degrading matrices were essentially obliterated (Figure 1A). Cell-seeded scaffolds implanted perivascular to the injured murine carotid artery demonstrated similar trends to *in vitro* degradation (Figure 1B). Injury increased degradation and the presence of cells retarded injury-mediated degradation and further stabilized matrices (Figure 1C), possibly due to increased local inflammation-mediated proteolysis. Cell viability and scaffold degradation were followed

using *in vivo* imaging. All ECs were lost 8 days after implantation but viability doubled in the slow degrading devices (p < 0.05, Figure 1D). Assuming that cell viability numbers below 10% were negligible in efficacy, we correlated effective cell viability with remaining material mass. Across all three material types, we observed a strong linear correlation, suggesting cell viability was tightly connected with the remaining scaffold mass (Figure 1E).

2.2. Differentially degrading scaffolds support cell engraftment and proliferation

Despite differences in pore size (Figure 2A–B) and mechanical properties (Figure 2C) we ensured that all scaffolds bore the same number of ECs at baseline (Figure 2 D–E), and prior to implantation (Figure S1). Increasing mechanical modulus was associated with a decrease in pore size (Figure S2), which was correlated with an increase in cell viability *in vivo* (Figure 1D), but no change in cell number *in vitro* (Figure S1). Image analysis of cell area of embedded ECs in different scaffolds showed no statistically significant change in cell morphology across scaffold conditions (Figure 1E, p > 0.05).

We assessed the *in vitro* capacity of MEECs cultured on differentially degrading scaffolds to inhibit human aortic smooth muscle cell (HASMC) proliferation as a model of the therapeutic effects of MEECs *in vivo*. Devices all significantly inhibited HASMC proliferation in a manner correlated with degradation rate (p < 0.05, cf. controls and each other) (Figure 3A). MEECs in slow-degrading scaffolds expressed detectable levels of matrix metalloproteinase-9 (MMP-9) while standard and fast-degrading scaffolds did not (p < 0.05). As MMP-9 can readily degrade denatured collagen, this may be indicative of a cell-mediated remodeling of the matrix itself. This remodeling may be driven by the higher stiffness of slow-degrading scaffolds. Additionally, MEECS in fast-degrading scaffolds expressed lower levels of interleukin-6 (IL-6), a potent cytokine involved in regulating the inflammatory response to vascular injury (p < 0.05, significance between fast-degrading scaffolds and other treatment conditions). Although MEECs in native and slow-degrading scaffolds expressed significantly higher levels of PECAM-1 than fast-degrading scaffolds (p < 0.05, fast-degrading versus other conditions), the levels were near the detection limit of the assay and were not judged to be meaningful. Remarkably, MEECs in different scaffolds did not show any significant differences in expression across the remaining range of inflammatory and ECM-modifying proteins tested (Figure 3B).

2.3. Improved endothelialization and reduced SMC hyperplasia and inflammation in MEEC-treated vascular injury

We hypothesized that the observed *in vitro* reduction in SMC proliferation and changes in MEEC secretome could result in functional improvements in vascular structure subsequent to injury. During wire injury, mouse carotids were denuded of endothelial cells, and an early inflammatory response was detected. By five days, smooth muscle cell hyperplasia was evident along with continued inflammation and only modest endothelial recovery. After 14 days, the vessel response had matured but remained diseased with a sustained intimal thickening. MEECs reduced inflammation at all time points, minimized SMC hyperplasia, and enhanced endothelialization, again in a manner dependent on matrix degradation (Figure 4A). Treatment with acellular scaffolds or free cells did not show improvements over untreated controls at 14 days (Figure S3).

Histological scoring of endothelialization and smooth muscle cell proliferation confirmed dependence on degradation rate. Endothelial recovery after injury was maximized for the slow degrading matrices and in this model there was no detectable decrease in smooth muscle cell proliferation except for the matrices with longest *in vivo* persistence (Figure 4B–C). Notably, the fast-degrading scaffolds exhibited equal or inferior performance to injury-only controls, possibly due to the inflammatory microenvironment causing MEECs to shift away from a reparative phenotype and towards a pathological one. These endothelialization and SMC hyperplasia results correlated with the local tissue inflammatory response detected after tail-vein injection of a fluorescent reporter of cathepsin B (Figure 5A). The acellular matrices had an insignificant effect on cathepsin B activity but cellular matrices reduced local vascular inflammation, with the greatest reduction for the slowest degrading devices (p < 0.05, Figure 5B, Figure S4). Longer-lasting scaffolds improve inflammatory modulation, likely through a combination of increased EC viability leading to reduced immune cell activation as well as modified cell-substrate interactions leading to critical changes in cell phenotype.

3. Discussion

Material design is known to be of paramount importance in determining the phenotype of endothelial cells. Embedding endothelial cells in appropriately designed biomaterial scaffolds causes the cells to adopt a healthy, reparative phenotype that reduces inflammation, immune responses, and tissue hyperplasia following a vascular injury, likely through paracrine effects on the surrounding tissue[4, 10, 11]. Our goal was to determine if these therapeutic effects of MEECs could be improved through changing the material properties. This study demonstrates that control over scaffold crosslinking could modulate these critical cell-substrate interactions and tune the reparative phenotype of matrix-embedded endothelial cells.

Cell behavior in 3D scaffolds has been shown to be highly dependent on surface chemistry, mechanical properties, pore size, and degradation rate[12, 13, 14]. Previous work on endothelial cells has elucidated some scaffold properties that are critical determinants of EC function. Extensive studies[15] have shown that mechanical stiffness of matrices have profound effects on the ability of ECs to form new capillary networks[16]. A series of elegant experiments has demonstrated that EC survival and proliferation on a fibronectin-coated surface is linked to a total cell area (i.e. a spread morphology) and *not* to ligand density, suggesting that matrix-induced changes in cell morphology can have significant effects on EC biology[14]. EC morphology and behavior has also been shown to be dependent on scaffold pore size, chemistry, and degradation rate[12, 17], though these effects have not been as well explicated. While the effects of scaffold properties on angiogenesis and EC survival and morphology have been studied in detail, fewer studies have focused on other aspects of EC function such as its immunomodulatory role and interactions with other cells. Glycation of collagen surfaces was shown to reduce FAK activation and NO release of ECs cultured under flow, and limit EC alignment during cyclic strain[18, 19]. In addition, ECs on glycated collagen surfaces exhibited increased permeability due to disrupted cell-cell interactions, which were attributed to changes in integrin binding and expression[19].

Previously, we have shown that culture of ECs inside collagen scaffolds of varying mechanics has significant effects on cell functionality *in vitro*. Cells embedded in more highly crosslinked matrices were able to inhibit SMC proliferation mediated through increased secretion of heparin sulfate proteoglycan. Higher stiffness also led to EC-mediated inhibition of T cell proliferation and increased expression of MMP inhibitors[11]. These phenotypic changes were tied to variations in the amount though not composition of ECM deposition in the scaffolds and variable integrin expression. These differentially crosslinked scaffolds also exhibited a range of other changes in physicochemical properties, though these were not examined; furthermore, the study was not extended to an *in vivo* vascular repair model. We hypothesized that EC functionality in treating vascular injury *in vivo* could be tuned by changing scaffold properties.

Here, we looked directly at the role of scaffold degradation in controlling EC functionality in a vascular injury model *in vivo*. We demonstrate that slower degrading scaffolds, which exhibit smaller pore size and stiffer bulk mechanics but no observable changes in cell morphology, were able to support increased cell viability in an *in vivo* carotid injury animal model. ECs in degradation-tuned scaffolds were able to differentially inhibit SMC proliferation and had altered IL-6 and MMP-9 expression, though most of their biosecretory profiles were unchanged. When implanted *in vivo*, cell-laden scaffolds were able to attenuate the inflammatory response following vascular injury in a degradation rate responsive manner, with attendant changes in endothelial recovery and SMC hyperplasia. These data suggest a strong therapeutic role for MEECs in potentiating vascular repair that can be tuned through manipulation of scaffold properties. Understanding the precise mechanism of the *in vivo* response is complicated by the range of physicochemical scaffold properties that changed from condition to condition, including degradation rate, mechanical stiffness, and pore size. Based on the aforementioned literature, we believe all of these factors are likely important in affecting EC-substrate interactions. During the course of tuning scaffold properties, it is inevitable that a variety of physicochemical factors will change; only in highly artificial controlled studies have previous studies been able to separate these effects[14]. In contrast, we present here a clinically relevant method of tuning scaffold properties to affect cell-substrate interactions. Changes in material properties are characterized in detail, and the resulting phenotypic response is evaluated by real-time monitoring of *in vivo* models. These results reveal an intricate interplay of scaffold properties and cell phenotype influencing each other, which in turn have profound effects on the surrounding tissue. We hypothesize that a key determinant of the differential biological response was the prolonged and increased viability of embedded cells in slower-degrading scaffolds, evidenced by the strong correlation between remaining scaffold mass and cell viability. Understanding the mechanism of this effect is challenging, but we believe that the inflammatory *in vivo* injury environment is fundamentally hostile to EC survival. The slower-degrading scaffolds may have protected EC viability through enhanced duration of EC-substrate interactions, lower porosity leading to a relatively privileged cellular microenvironment, or changes in mechanotransduction signals leading to altered EC modulation of its surroundings. This increased viability enhanced the exposure time to the anti-inflammatory effects of MEECs, changing healing outcomes. We hypothesize that

MEECs were able to stimulate re-endothelialization of the damaged vessel, which in turn had potent effects on inflammation and tissue state.

Scaffold degradation rates *in vivo* are likely dependent on the expression of matrix degrading enzymes by inflammatory cells, matrix remodeling by engrafted endothelial cells, and mechanical stresses. This intricate interplay involves feedback loops between the embedded endothelial cell secretome, the level of inflammation, and the cell substrate interactions. Tweaking the initial cell-substrate interactions and its subsequent degradation rate can have significant effects on cell viability and phenotype. We hypothesize that this cell-mediated mechanism of slower scaffold degradation is due to modulation of the inflammatory tissue response following vascular injury. Previous studies have shown a potent effect of MEECs on inflammatory and immune responses; here, we showed that slower degradation kinetics, with its attendant increased cell viability, was able to further reduce the inflammatory response to vascular injury *in vivo* over 12 days. These effects persist even after the degradation of most of the scaffold and loss of cells; reduced inflammation was seen even though cell viability had largely disappeared after a week *in vivo*.

The therapeutic effect of MEECs may cause longer-term changes to the secretome of cells in the surrounding tissues, leaving a healthier tissue even after scaffold degradation. *In vitro* co-culture of MEECs with SMCs showed significant inhibition of SMC proliferation in a degradation rate dependent manner. Further *in vitro* analysis of the matrix-embedded HAEC secretome suggests that the different scaffolds result in changes to cell phenotype, notably increasing secretion of both IL-6 and MMP-9 for slower-degrading scaffolds. The increased expression of IL-6 for scaffolds which demonstrated reduced inflammation *in vivo* and SMC proliferation *in vitro* appears initially paradoxical, given that it is normally assumed to be a pro-inflammatory cytokine that increases SMC growth[20]. However, recent research has demonstrated multiple signaling modalities for IL-6 depending on its interaction with IL-6R in either membrane bound or soluble form. These different modalities have been shown to modulate whether IL-6 signaling is pro- or anti-inflammatory, though the details have yet to be fully elucidated[21]. Further investigation of the expression of proteins involved in this modulation is necessary to help confirm its role as an anti-inflammatory cytokine *in vivo*. Similarly, the increased secretion of MMP-9 by slower degrading (and thus SMC-inhibitory) scaffolds hints at a complex interaction between matrix remodeling and cellular behavior. Previous studies have demonstrated MMP-9 to have a potent role in enhancing SMC proliferation and migration following vascular injury, making the correlation of its increased expression with reduced SMC proliferation ambiguous[22, 23]. We must also consider that MEECs secrete a plethora of cytokines and chemokines, many of which were not measured here, so MMP-9 function alone may not explain the MSC response. However, while MMP-9 secretion by SMCs is likely important in neointima formation, it also has a significant role in the organization of adventitial collagen and modulation of cell-substrate interactions[23]. The observed increase in MMP-9 secretion may thus be tied not to SMC proliferation but rather to the embedded HAECs 'tuning' their surrounding matrix. Substrate stiffness has long been tied to expression of MMPs and other matrix remodeling proteins, with increasing stiffness often causing upregulation of MMPs[24]. Additionally, endothelial progenitor cells seeded in a gelatin-hyaluronan hydrogel increased MMP expression at higher stiffnesses up to 650

Pa[25]. Gelfoam-embedded HAECs likely upregulated MMP-9 activity in response to the higher substrate stiffness of the crosslinked, slow-degrading matrix. These changes in the HAEC secretome in differentially degrading scaffolds hint at a multifaceted interaction of factors controlled by cell-substrate interactions that can modulate their reparative phenotype. In this study, we used a mouse carotid wire injury model as a method of mimicking intimal lesions in the vascular endothelium common following vascular interventions such as stenting. This model was particularly well suited to evaluating EC-material interactions in potentiating vascular repair. Using a small animal model allowed us to noninvasively track material degradation, tissue inflammation, and cell viability in real time using IVIS, offering an unprecedented opportunity to obtain spatial and temporal resolution in studying cell-material-tissue interactions. The type of injury created by wire denudation of the epithelium matched expected injuries following stenting, with the attendant inflammation, SMC hyperplasia, and re-endothelialization over time[26]. Limitations of this model, however, include the relatively rapid re-endothelialization of untreated controls (which does not occur in rat balloon injury models) and the relatively minor insult to the media, potentially decreasing the SMC response. Nevertheless, it allowed us to probe the acute response to vascular injury and its remediation by MEECs as a function of degradation rate.

4. Conclusion

Matrix-embedded endothelial cells have been previously described as a promising therapeutic method to reduce inflammation and intimal hyperplasia following vascular injury. Here, we focused on the role of material design in tuning the therapeutic effect of MEECs. We demonstrate that cell-substrate interactions can be controlled by varying the crosslinking (and hence degradation rate, mechanics, and pore size) of standard compressed collagen scaffolds. Using a novel mouse carotid wire injury model and sophisticated *in vivo* imaging techniques, we were able to track scaffold degradation, cell viability, and local inflammation in real time. Control of compressed collagen scaffold degradation *in vitro* and *in vivo* was dependent on disease state and ECs. Vascular injury increased degradation and the presence of cells retarded degradation and further stabilized matrices. Slower-degrading scaffolds were shown to reduce SMC proliferation *in vitro,* protect against loss of cell viability *in vivo*, reduce injury-related inflammation *in vivo* and improve endothelialization and SMC hyperplasia. This is likely the result of changes in the scaffold mechanics and degradation rate that modulated the endothelial cell secretome, especially that of IL-6 and MMP-9. These data demonstrate that material properties can be controlled to tune the reparative outcomes of cell-based therapeutics.

5. Experimental Section

Synthesis of scaffolds with differential degradation rates

Standard scaffolds (Gelfoam compressed sponge, Pfizer) were cut to 2×4×6 mm blocks and used as received. To create slow-degrading matrices, standard blocks were chemically crosslinked using carbodiimide chemistry. 1-Ethyl-3-(3-dimethylaminopropyl)carbodiimide (EDC, Sigma) was dissolved at 54 mM in phosphate buffered saline (PBS, Lonza) with 22 mM N-hydroxysuccinimide (NHS, Sigma). This EDC/NHS crosslinker solution was added

to blocks (10 ml of crosslinker solution for 5 scaffolds) and agitated for three hours at room temperature, forming amide bond crosslinks within the material. Following crosslinking, slow-degrading matrices were thoroughly washed in PBS and stored in Endothelial Growth Medium-2 (EGM-2, Lonza) overnight before use. Fast-degrading scaffolds were produced by partial enzymatic degradation of standard matrices. A range of collagenase type 4 (Worthington Biochemical) concentrations in PBS (0.001 mg/ml, 0.01 mg/ml, 0.1 mg/ml, and 1 mg/ml) were prepared and added to scaffolds incubated at 37° C (90% humidity, 5% CO_2) for periods ranging from 10 to 60 minutes. Subsequently, scaffolds were thoroughly washed in PBS and stored overnight in EGM-2 media prior to use.

In vitro mechanical analysis of scaffolds

Scaffolds with different degradation kinetics were cut to 9×8×2 mm blocks, measured by digital micrometers, and placed in an Instron E3000 uniaxial mechanical tester between two unlubricated, nonporous compression platens. An unconfined compression test was performed at 0.5%/s until 20% strain; scaffolds were immersed in PBS throughout the test to mimic implantation conditions. The resultant normal force was measured using a 10 N load cell (Instron). Engineering stress in the normal direction and axial strain were calculated based on initial material geometry, using an assumption of constant cross-sectional area. Compressive modulus was calculated from the linear portion of the stress-strain curve, approximately 5–20% strain.

In vitro degradation kinetics

Matrix blocks were labeled with fluorescent tags to enable degradation tracking *in vitro* and *in vivo*. A succinimidyl ester of Texas Red-X (Invitrogen) was dissolved in dimethyl sulfoxide to 10 mg/ml. Each block was immersed in 320 μl of 200 mM sodium bicarbonate to which 0.93 μl of Texas Red X concentrate was added. The reaction proceeded at room temperature for 1 hour, after which scaffolds were washed thoroughly in PBS to remove unreacted fluorophore. Scaffolds were incubated in EGM-2 supplemented media for ten days changed daily and assessed for fluorescent signal on a Varioskan Flash fluorescent plate reader (excitation filter: 605 nm, emission filter: 660 nm, Thermo Scientific). After ten days, *in vivo* implantation was simulated by the addition of 30 μl of a 0.25 μg/l collagenase solution for an additional five days. It was determined that a single fast-degrading matrix condition (0.01 mg/ml collagenase reacted for 1 hour) exhibited similar cell number to native and slow-degrading scaffolds for the entire 10 days of pre-implantation cell culture and this condition was chosen for all further experiments (Figure S1).

Cell seeding onto scaffolds

Human aortic endothelial cells (HAECs) isolated and pooled from healthy 20–25 year old adult donors (Promocell) were maintained at 37° C in 90% humidity and 5% CO2 and cultured for up to 6 passages in Endothelial Growth Medium 2 (EGM-2, Lonza) supplemented with 10% fetal bovine serum (Gibco) and 1% penicillin/streptomycin (Lonza). Prior to cell seeding, all matrix formulations were tagged with Texas Red-X and incubated in 5 ml EGM-2 supplemented media overnight. Each scaffold was seeded with 10^5 cells by applying a 20 μl suspension of $5×10^4$ HAECs to either side of the scaffold[7]. After seeding, scaffolds were incubated at 37° C and the cells were allowed to infiltrate and adhere for 1

hour. Groups of three cell-seeded matrices were placed in a freestanding centrifuge tube containing 5 ml of EGM-2 supplemented media and incubated for 10 days. Growth medium was changed every 48 hours and after 10 days, scaffolds were fully degraded by digestion in varying concentrations of collagenase for 1 hour (1 mg/ml for fast-degrading and standard matrices, 4 mg/ml for crosslinked slow-degrading devices). Cell number was determined at periodic intervals using a hemacytometer and viability by trypan blue exclusion under microscopy.

Secretion of inflammation-modulating cytokines and matrix remodeling proteins by MEECs was evaluated using a protein expression array. Cell-laden scaffolds were incubated for 10 days in EGM-2 supplemented media to reach maximal cell number, with media changes every 2 days. Following the 10 day incubation, 8 scaffolds of each type were incubated in 1.5 ml of EGM-2 supplemented media in freestanding tubes for 48 hours. Subsequently, the tubes were centrifuged and the conditioned media were collected and analyzed using the RayBio Human Angiogenesis Antibody Array C series 1000 protein array, which tests for a variety of vascular-related inflammatory and matrix remodeling proteins. EGM-2 supplemented medium was used as a negative control.

Engineering HAECs for *in vivo* cell tracking

In vivo cell tracking of HAECs was accomplished by transduction with the pMMP-LucNeo retrovirus using Polybrene at 8 ug/ml as previously described[27]. Cells expressing luciferase were selected for by growth in media containing G418 500 ug/ml. Luminescence measurements *in vitro* (Varioskan Flash plate reader) and following implantation *in vivo* (IVIS Spectrum) were confirmed to be linearly correlated with cell number as determined by hemacytometry of cells from degraded matrices.

In vitro smooth muscle cell inhibition assay

Human aortic smooth muscle cells (HASMCs) were seeded on 6-well plates (10^4 cells/well) and then exposed to HAECs seeded on fast, native, and slow-degrading matrices in Transwell inserts (0.4 μm pores, Corning). The ECs had been cultured in EGM-2 supplemented media for nine days. EGM-2 supplemented media (1.5 ml) and 8 HAEC-embedded scaffolds were added to each insert. To mimic *in vivo* degradation, 100 μl of 0.1 mg/ml collagenase was applied to each well daily. On the desired day following the commencement of co-culture (4 and 7 days), the HASMCs were counted and compared to controls without co-culture.

Wire injury model and *in vivo* implantation of scaffolds

All animal procedures were approved by the Committee on Animal Care at the Massachusetts Institute of Technology (protocol #0412-032-15) and follow the National Institutes of Health guidelines for animal care. SKH-1 hairless male mice (Charles River) were used at 6 weeks of age; the strain is euthymic and immunocompetent, and was chosen to improve *in vivo* imaging of fluorescent implants. The right carotid artery was isolated, clamped, and a small incision was made on the internal carotid. A 0.01 inch diameter guidewire (SilverSpeed hydrophilic guidewire, Covidien) was inserted and retracted thrice to denude the endothelial layer of the artery. The incision was closed and single scaffolds were

gently placed around the injured vessel. A video of the carotid wire injury model can be seen in Figure S5. Conditions included HAEC-seeded scaffolds with different degradation rates (n=22 animals, 8 fast-degrading, 6 standard, 8 slow-degrading), acellular scaffolds (n=23 animals, 8 fast-degrading, 7 standard, 8 slow-degrading), free HAECs (n=7 animals), and injury alone without cells or matrices (n=6 animals). Additionally, the differentially degrading scaffolds were placed perivascularly to healthy right carotid arteries for non-injured controls (n=25 animals, 9 fast-degrading, 7 standard, 9 fast-degrading).

In vivo tracking

Periodic imaging of devices with Texas-Red labelled matrices and luciferase-expressing HAECs in intact animals providing continuous signal of matrix fate was performed with an In Vivo Imaging System (IVIS Spectrum, Perkin Elmer). An excitation filter of 605 nm and an emission filter of 660 nm was used for the former and intraperitoneal injection of luciferin solution (30 mg/ml Perkin Elmer) 15 minutes prior to imaging for the latter. The inflammatory response to injury was measured *in vivo* using Cathepsin B 680 FAST (Perkin Elmer) injected IV (100 ul PBS, 24 nmol). This dye is composed of a pair of quenched fluorophores separated by a Cathepsin B-sensitive peptide and only fluoresces upon cleavage of this linker peptide by Cathepsin B. Twenty hours after injection, the mice were imaged using IVIS (excitation: 675 nm, emission: 720 nm) to determine localization and extent of cathepsin B activity every four days.

Histological analysis

Two weeks after surgery, mice were euthanized and perfused via the left ventricle with 4% paraformaldehyde following a saline flush. Carotid arteries were excised with any remaining scaffold material and fixed in 5 ml of 4% PFA at 4 C. The injured vessel area was extracted, paraffin-embedded, sectioned to 5 μm from the proximal, middle, and distal elements and stained with VerHoeff's elastin stain and H&E. Morphometric analysis to determine the degree of endothelialization was performed on all segments.

Statistics

Data are shown as mean with standard deviation. Statistical analyses were performed using MATLAB with ANOVA followed by a multiple comparisons procedure using the Tukey's Honestly Significant Difference post-hoc test with an alpha value of 0.05. Repeated measures data (including material degradation, cell viability, and inflammation data) was analyzed in JMP statistical software. We used a mixed effects linear model with an autoregressive (order 1) covariance structure.

Supplementary Material

Refer to Web version on PubMed Central for supplementary material.

Acknowledgments

References

1. Kienstra KA, Hirschi KK. Methods Mol Biol. 2012; 904:155. [PubMed: 22890930] Critser PJ, Voytik-Harbin SL, Yoder MC. Cell Prolif. 2011; 44(Suppl 1):15. [PubMed: 21481038]

2. Nathan A, Nugent MA, Edelman ER. Proc Natl Acad Sci U S A. 1995; 92:8130. [PubMed: 7667257] Nugent HM, Edelman ER. J Surg Res. 2001; 99:228. [PubMed: 11469891]

3. Patel SD, Waltham M, Wadoodi A, Burnand KG, Smith A. Ther Adv Cardiovasc Dis. 2010; 4:129. [PubMed: 20200200]

4. Nugent MA, Nugent HM, Iozzo RV, Sanchack K, Edelman ER. Proc Natl Acad Sci U S A. 2000; 97:6722. [PubMed: 10841569]

5. Methe H, Hess S, Edelman ER. Thromb Haemost. 2007; 98:278. [PubMed: 17721607]

6. Alexander I, Edelman ER, Methe H. Cell Transplant. 2009; 18:255. [PubMed: 19558774] Methe H, Hess S, Edelman ER. Semin Immunol. 2008; 20:117. [PubMed: 18243732] Methe H, Edelman ER. Circulation. 2006; 114:I233. [PubMed: 16820578]

7. Indolfi L, Baker AB, Edelman ER. Biomaterials. 2012; 33:7019. [PubMed: 22796162]

8. Grewe PH, Deneke T, Machraoui A, Barmeyer J, Muller KM. J Am Coll Cardiol. 2000; 35:157. [PubMed: 10636274] Farb A, Sangiorgi G, Carter AJ, Walley VM, Edwards WD, Schwartz RS, Virmani R. Circulation. 1999; 99:44. [PubMed: 9884378] Schwartz RS, Henry TD. Rev Cardiovasc Med. 2002; 3(Suppl 5):S4. [PubMed: 12478229]

9. Artzi N, Oliva N, Puron C, Shitreet S, Artzi S, bon Ramos A, Groothuis A, Sahagian G, Edelman ER. Nat Mater. 2011; 10:704. [PubMed: 21857678]

10. Methe H, Nugent HM, Groothuis A, Seifert P, Sayegh MH, Edelman ER. Circulation. 2005; 112:I89. [PubMed: 16159871] Nugent HM, Sjin RT, White D, Milton LG, Manson RJ, Lawson JH, Edelman ER. J Vasc Surg. 2007; 46:548. [PubMed: 17826244] Methe H, Hess S, Edelman ER. Eur J Immunol. 2007; 37:1773. [PubMed: 17559179] Methe H, Edelman ER. Transplant Proc. 2006; 38:3293. [PubMed: 17175253] Methe H, Groothuis A, Sayegh MH, Edelman ER. Faseb J. 2007; 21:1515. [PubMed: 17264166] Hess S, Methe H, Kim JO, Edelman ER. Cell Transplant. 2009; 18:261. [PubMed: 19558775]

11. Murikipudi S, Methe H, Edelman ER. Biomaterials. 2013; 34:677. [PubMed: 23102623]

12. Sung HJ, Meredith C, Johnson C, Galis ZS. Biomaterials. 2004; 25:5735. [PubMed: 15147819]

13. Cukierman E, Pankov R, Stevens DR, Yamada KM. Science. 2001; 294:1708. [PubMed: 11721053] Engler AJ, Sen S, Sweeney HL, Discher DE. Cell. 2006; 126:677. [PubMed: 16923388] Discher DE, Janmey P, Wang YL. Science. 2005; 310:1139. [PubMed: 16293750] Liu H, Liu X, Meng J, Zhang P, Yang G, Su B, Sun K, Chen L, Han D, Wang S, Jiang L. Adv Mater. 2013; 25:922. [PubMed: 23161781] Liu H, Li Y, Sun K, Fan J, Zhang P, Meng J, Wang S, Jiang L. Journal of the American Chemical Society. 2013; 135:7603. [PubMed: 23601154]

14. Chen CS, Mrksich M, Huang S, Whitesides GM, Ingber DE. Science. 1997; 276:1425. [PubMed: 9162012]

15. Califano JP, Reinhart-King CA. J Biomech. 2010; 43:79. [PubMed: 19815215] Francis ME, Uriel S, Brey EM. Tissue Eng Part B Rev. 2008; 14:19. [PubMed: 18454632]

16. Sieminski AL, Hebbel RP, Gooch KJ. Exp Cell Res. 2004; 297:574. [PubMed: 15212957] Mason BN, Starchenko A, Williams RM, Bonassar LJ, Reinhart-King CA. Acta Biomater. 2013; 9:4635. [PubMed: 22902816] Yamamura N, Sudo R, Ikeda M, Tanishita K. Tissue Eng. 2007; 13:1443. [PubMed: 17518745] Deroanne CF, Lapiere CM, Nusgens BV. Cardiovasc Res. 2001; 49:647. [PubMed: 11166278]

17. Zeltinger J, Sherwood JK, Graham DA, Mueller R, Griffith LG. Tissue Eng. 2001; 7:557. [PubMed: 11694190] Cuy JL, Beckstead BL, Brown CD, Hoffman AS, Giachelli CM. J Biomed Mater Res A. 2003; 67:538. [PubMed: 14566796] Tidwell CD, Ertel SI, Ratner BD, Tarasevich BJ, Atre S, Allara DL. Langmuir. 1997; 13:3404.

18. Kemeny SF, Figueroa DS, Andrews AM, Barbee KA, Clyne AM. J Biomech. 2011; 44:1927. [PubMed: 21555127]

19. Figueroa D, Kemeny S, Clyne A. Cel Mol Bioeng. 2011; 4:220.

20. Ikeda U, Ikeda M, Oohara T, Oguchi A, Kamitani T, Tsuruya Y, Kano S. Am J Physiol. 1991; 260:H1713. [PubMed: 1709793]

21. Scheller J, Garbers C, Rose-John S. Semin Immunol. 2013

22. Cho A, Reidy MA. Circ Res. 2002; 91:845. [PubMed: 12411400]

23. Galis ZS, Johnson C, Godin D, Magid R, Shipley JM, Senior RM, Ivan E. Circ Res. 2002; 91:852. [PubMed: 12411401]

24. Petersen A, Joly P, Bergmann C, Korus G, Duda GN. Tissue Eng Part A. 2012; 18:1804. [PubMed: 22519582]

25. Hanjaya-Putra D, Yee J, Ceci D, Truitt R, Yee D, Gerecht S. J Cell Mol Med. 2010; 14:2436. [PubMed: 19968735]

26. Lindner V, Fingerle J, Reidy MA. Circ Res. 1993; 73:792. [PubMed: 8403250]

27. Rubin JB, Kung AL, Klein RS, Chan JA, Sun Y, Schmidt K, Kieran MW, Luster AD, Segal RA. Proc Natl Acad Sci U S A. 2003; 100:13513. [PubMed: 14595012]
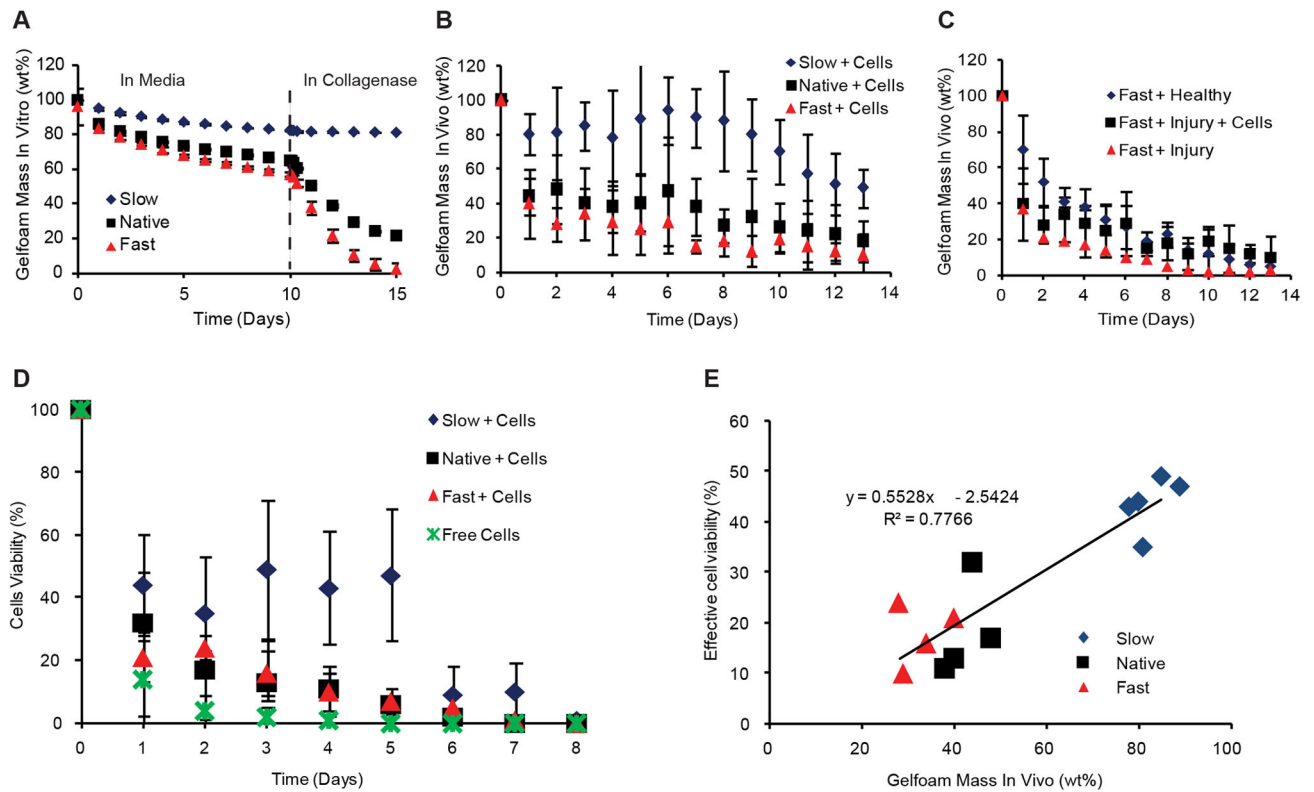
Figure 1. Scaffold Degradation *in vitro* and *in vivo*

Acellular scaffolds degraded *in vitro* differentially during culture in media for 10 days followed by culture in collagenase for 5 days to mimic *in vivo* implantation ($p < 0.05$, significant differences between all treatment levels) (A). *In vivo* imaging was used to detect fluorescently-tagged scaffolds *in situ* in real time demonstrating different degradation rates of cell-seeded scaffolds in injured mice ($p < 0.05$, significant differences between all treatment levels) (B). Upon induction of vascular injury using a carotid wire injury model, degradation rates of fast-degrading scaffolds without seeded cells were faster than healthy controls, but addition of cells slowed degradation ($p < 0.05$, injured acellular scaffolds vs. other conditions; healthy vs. cellular injured was not significant) (C). Cell viability in an injured perivascular environment over 9 days *in vivo* was assessed for each scaffold and compared to free cells, showing increased viability for cells in slow-degrading scaffolds ($p < 0.05$, significance between slow-degrading scaffolds and all other conditions) (D). Effective viability (>10%) was closely correlated with remaining scaffold mass across treatment conditions (E).
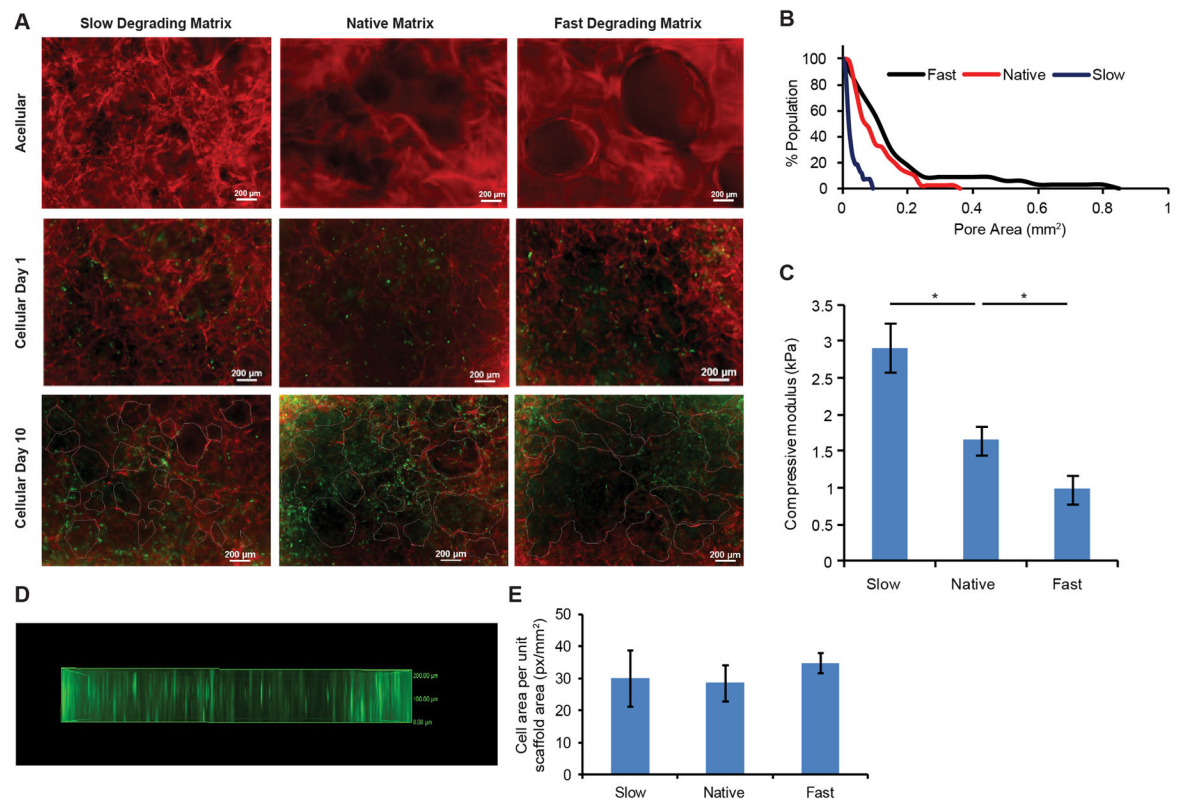
Figure 2. Cell-material interactions in differentially degrading scaffolds

Fluorescently tagged HAECs (green) were successfully seeded onto scaffolds, and proliferated over 10 days of *in vitro* culture (A; approximate pore boundaries outlined at 10 days). Pore sizes of the different scaffolds varied with degradation rate (B). Scaffolds exhibited differential bulk mechanical properties (*, $p < 0.05$) (C). Z-stack images of cell-seeded scaffolds show a relatively uniform distribution of cells throughout the scaffold (fast-degrading scaffold shown as an example) (D); cell morphology determined by image analysis after seeding was not statistically different across the scaffold types ($p = 0.19$) (E).
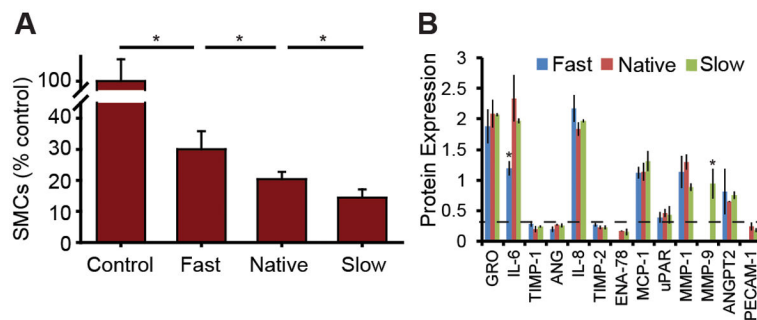
Figure 3. *In vitro* assessment of cell phenotype in differentially degrading scaffolds
SMC proliferation was inhibited by MEECs in a degradation-rate dependent manner (p < 0.05, differences between all scaffold conditions and controls) (A). MEEC secretion of MMP-9 and IL-6 was significantly different, while other biosecretory proteins were unchanged (*, p < 0.05; effective detection threshold of 30% at dashed line) (B).
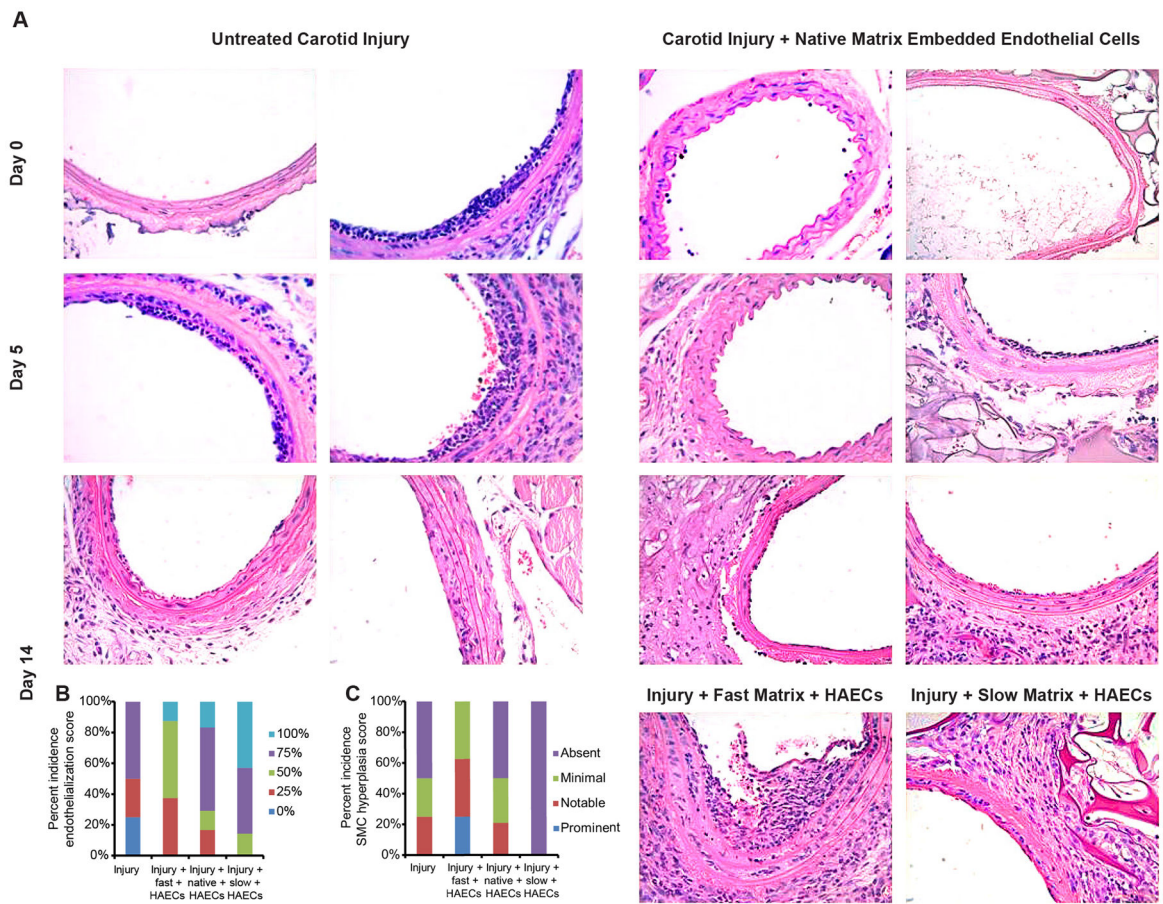
Figure 4. Functional outcomes of in vivo implantation of cell-seeded devices

H&E images of murine carotid arteries 0, 5 and 14 days after intervention (A).

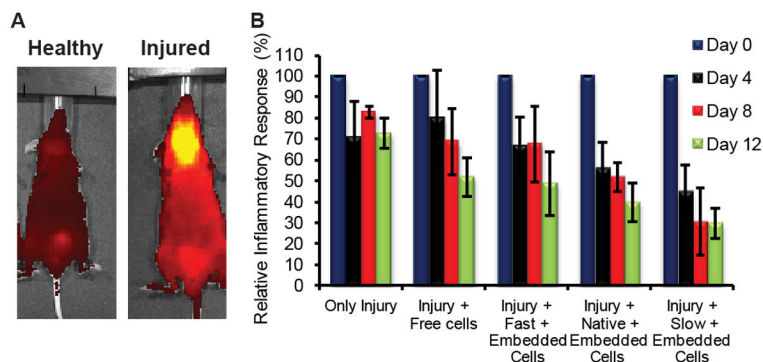Quantification of endothelial recovery (B) and SMC proliferation (C).

Figure 5. Modulation of inflammation *in vivo*
Inflammation following vascular injury was tracked using a cathepsin B-sensitive fluorescent dye (A). Slower degrading cellular scaffolds showed significant decreases in inflammation over 12 days relative to post-injury inflammation ($p < 0.05$, significance between slow scaffolds and controls, free cells, and fast-degrading; significance between standard scaffolds and controls at this power level) (B). **Collagen matrix-embedded endothelial cells** are a potent modulator of the healing blood vessel following injury. Varying scaffold degradation rates and other material properties can have significant effects on cell viability and therapeutic function *in vivo.* Real time tracking of local inflammation, cell viability, and material degradation *in vivo* allows an unprecedented window into the dynamics of cell-scaffold-microenvironment interactions.